

# Timescale of twin-peak quasi-periodic oscillations and mass of accreting neutron stars

Gabriel Török<sup>1\*</sup>, Kateřina Goluchová<sup>1</sup>, Eva Šrámková<sup>1</sup>,  
Martin Urbanec<sup>1</sup>, Odele Straub<sup>1,2</sup>

<sup>1</sup> *Institute of Physics and Research Centre for Computational Physics and Data Processing,  
Silesian University in Opava, Bezručovo nám. 13, CZ-746 01 Opava, Czech Republic*

<sup>2</sup> *Max Planck Institute for extraterrestrial Physics, Gießenbachstraße 1, 85748 Garching, Germany*

## ABSTRACT

Einstein’s general relativity predicts that orbital motion of accreted gas approaching a neutron star (NS) in a NS low-mass X-ray binary (LMXB) system occurs on a time scale proportional to the NS mass. Radiation of the gas accounts for most of the observed LMXBs variability. In more than a dozen of sources twin-peak quasi-periodic oscillations (QPOs) have been observed. Inspired by the expected proportionality between periods of orbital motion and NS mass we present a straightforward comparison among these sources. We investigate relations between QPO periods and their ratios and identify characteristic time scales of QPOs associated to individual sources. These timescales are likely determined by the relative mass of each NS. We show that the characteristic time scale of the millisecond pulsar XTE J1807.4-294 is longer than for most other NS LMXBs. Consequently, models of QPOs that consider geodesic orbital frequencies imply that the X-ray pulsars’ mass has to be about 50% higher than the average mass of other sources. Consideration of other X-ray pulsars indicates that the exceptionality of XTE J1807.4-294 cannot be related to NS magnetic field in any simple manner. We suggest that QPOs observed in this source can help to discriminate between the proposed versions of the NS equation of state.

**Key words:** X-Rays: Binaries — Accretion, Accretion Disks — Stars: Neutron

## 1 INTRODUCTION

Accreting relativistic compact objects provide a unique opportunity to observe effects associated with strong gravity in both black hole (BH) and neutron star (NS) systems (van der Klis 2006; McClintock & Remillard 2006a; Abramowicz & Fragile 2013). The latter systems may serve as a good tool for exploration of supra-dense matter (Weber 1999; Latimer & Prakash 2004). A large number of observations of X-ray radiation from NS Low-mass X-ray binaries (LMXBs) has been gathered over the past two decades. These systems exhibit a very complex phenomenology including distinct types of spectral behaviour and temporal variability. From the spectral evolution point of view, NS LMXBs are often classified as atoll- or Z- sources based on the shape of the track which they follow in the so-called colour-colour diagram (e.g. van der Klis 2006). While Z sources are generally more stable and brighter, atoll sources are weaker and show significant changes in the X-ray luminosity. In both types of sources, the power-density spectrum (PDS) that represents

their variability commonly include broad-band noise continuum with descending shape often accompanied by more or less sharp peaks.

Some of the sources, the accreting millisecond pulsars (AMXPS), pose very sharp peaks - X-ray pulsations - that are associated to NS rotation and the influence of NS magnetic field on the accreted matter. At present there is nevertheless no detailed consensus on the NS magnetic field strength in the accreting LMXBs. There is a general agreement that the surface dipole field at the NS stellar equator reaches values of  $B \sim 10^7 - 10^{10}$  G (Mukherjee et al. 2015). More detailed estimates are inferred from miscellaneous hypotheses of NS evolution and it is not even clear whether or not the X-ray pulsations can be linked to magnetic field more strongly than in other sources. In most cases the AMXPS belong among atoll sources that are believed to have magnetic fields that are weaker than for the Z-sources (Patruno & Watts 2012).

Less sharp peaks that often appear in the NS PDS are called quasi-periodic oscillations (QPOs). These are usually distinguished into groups of low- and high- frequency QPOs. The low frequency QPOs in NS sources have frequencies in

\* E-mail: gabriel.torok@gmail.com

the range of 1 – 100 Hz. In the case of Z-sources they have been further classified into horizontal, flaring, and normal branch oscillations (HBO, FBO, and NBO, respectively) depending on the position of the source in the colour-colour diagram. Oscillations with properties similar to HBOs have also been observed in several atoll sources (see [van der Klis 2006](#), for a review). The high-frequency (HF) QPOs in the NS sources span a frequency range of tens to more than thousands of hertz. They frequently appear in pairs that are observed simultaneously at frequencies  $\nu_U > \nu_L$ . Hence the name twin-peak QPOs by which they are commonly known. Sources that exhibit both X-ray pulsations and twin-peak QPOs are very rare, but they do exist.<sup>1</sup>

The strength of peaks that form the twin-peak QPOs expressed in terms of the fractional root-mean-squared (rms) amplitude,  $r$ , varies sometimes being as high as  $r \sim 30\%$ . The coherence of the signal may vary as well. There have been reported peaks with quality factor (centroid frequency of the peak divided by its full width at half maximum) of up to  $Q = 300$  ([Barret et al. 2005a](#); [Barret & Vaughan 2012](#)). Variable frequencies along with high coherence and high amplitude make NS HF QPOs different from the weak HF QPOs that are observed in BH sources (e.g. [Remillard et al. 2002](#); [McClintock & Remillard 2006b](#)). Those are associated with having stable frequencies that often form a 3:2 frequency ratio (first noticed by [Abramowicz & Kluźniak 2001](#)),

$$R \equiv \nu_U / \nu_L = 1.5. \quad (1)$$

However, see the works of [Belloni et al. \(2012\)](#), [Belloni & Altamirano \(2013\)](#) and [Varniere & Rodriguez \(2018\)](#) where the robustness of the 3:2 ratio is challenged.

Robust correlations are observed between the frequencies of twin-peak QPOs. Each source reveals its specific frequency correlation,  $\nu_U = \nu_U(\nu_L)$ , although the sources roughly follow a common pattern ([Psaltis et al. 1999](#); [Abramowicz et al. 2005b,a](#); [Zhang et al. 2006](#)). Despite the fact that QPOs have now been observed for more than three decades, the origin of both LF and HF QPOs is still poorly understood. There is presently no commonly accepted model for either BH or NS HF QPOs. On the other hand, based on several strong arguments, it is generally expected that these oscillations originate in orbital motion in the vicinity of the compact object.

## 2 ORBITAL MODELS OF QPOS

Various competing models of QPOs have been proposed. It is usually assumed that the QPO excitation occurs within the most luminous accretion region located less than two tens of Schwarzschild radii above the inner edge of the accretion disc. Several models suggest that QPOs are produced by a local motion of accreted inhomogeneities such as blobs or vortices. This subset of QPO models includes the so-called relativistic precession (RP) or tidal disruption (TD) model ([Abramowicz et al. 1992](#); [Stella & Vietri 1998b, 1999](#); [Čadež](#)

[et al. 2008](#); [Kostić et al. 2009](#); [Bakala et al. 2014](#); [Karssen et al. 2017](#); [Germanà 2017](#)).

Another possibility is to relate the QPOs to a collective motion of the accreted matter, in particular to oscillatory modes of an accretion disc ([Wagoner et al. 2001](#); [Rezzolla et al. 2003](#); [Abramowicz et al. 2006](#); [Ingram & Done 2010](#); [Fragile et al. 2016](#)). Such models often work with the idea of oscillations in a slender accretion torus and some sort of resonance between the torus oscillatory modes. An example is the epicyclic resonance (Ep) model proposed by [Kluźniak & Abramowicz \(2001\)](#). Several other models have been discussed by a large group of authors (see, e.g. [Alpar & Shaham 1985](#); [Lamb et al. 1985](#); [Miller et al. 1998](#); [Psaltis et al. 1999](#); [Wagoner 1999](#); [Psaltis & Norman 2000](#); [Wagoner et al. 2001](#); [Abramowicz & Kluźniak 2001](#); [Kluźniak & Abramowicz 2001](#); [Kato 2001](#); [Titarchuk & Wood 2002](#); [Abramowicz et al. 2003a,b](#); [Rezzolla et al. 2003](#); [Kluźniak et al. 2004](#); [Pétri 2005](#); [Zhang 2004, 2005](#); [Bursa 2005](#); [Török et al. 2007](#); [Kato 2007, 2008](#); [Stuchlík et al. 2008](#); [Čadež et al. 2008](#); [Kostić et al. 2009](#); [Germanà et al. 2009](#); [Mukhopadhyay 2009](#); [Stuchlík et al. 2013](#); [Stuchlík et al. 2014](#); [Török et al. 2016a](#); [Wang et al. 2015](#); [Stuchlík et al. 2015](#); [Shi & Li 2009](#); [Shi et al. 2018](#)).

### 2.1 Frequency relation associated to CT model

[Török et al. \(2018\)](#) have recently found and explored a surprisingly simple analytic relation that reproduces individual correlations for a group of several sources through a single parameter,

$$\nu_L = \nu_U \left( 1 - \mathcal{B} \sqrt{1 - (\nu_U / \nu_0)^{2/3}} \right), \quad (2)$$

where  $\nu_0$  equals to Keplerian frequency at the innermost stable circular orbit (ISCO),  $\nu_0 = \nu_{ISCO}$ , and  $\mathcal{B} = 0.8$ . In the Schwarzschild spacetime,  $\nu_{ISCO}$  is given solely by the NS mass  $M$ . The authors argue that relation (2) supports the hypothesis of the orbital origin of twin-peak QPOs. They discuss its interpretation in terms of global motion of the accreted fluid.

For  $\mathcal{B} = 1$  equation (2) describes predictions of the RP model, while the same relation provides predictions of a model that assumes an oscillating pressure-supported torus located at the innermost accretion region when  $\mathcal{B} = 0.8$ .<sup>2</sup> The torus is assumed to form a cusp by filling up its critical equipotential volume (see [Rezzolla et al. 2003](#); [Zanotti et al. 2005](#); [Török et al. 2016b](#); [de Avellar et al. 2018](#); [Török et al. 2018](#), for a further context). We refer to this model as to CT model. [Török et al. \(2018\)](#) have found that non-rotating NS mass inferred from equation (2) and  $\mathcal{B} = 0.8$  does not much vary across the individual sources; there is  $M < 2M_\odot$  except for the outstanding case of the XTE J1807.4-294 millisecond pulsar which is associated to high values of  $M$ ,  $M > 2.4M_\odot$ . In next we explore this finding and discuss its interpretation

<sup>1</sup> So far only three sources have displayed both, a number of twin-peak QPO detections, and strong X-ray pulsations ([Méndez & Belloni 2007](#); [Patruno & Watts 2012](#)). These sources are further considered within our paper - see Table 1 for the list of them.

<sup>2</sup> [Török et al. \(2018\)](#) have also investigated data fitting with  $\mathcal{B}$  being a free parameter further improving the fits in some sources. They discussed deviations from  $\mathcal{B} = 0.8$  in terms of non-geodesic effects other than the influence of the torus pressure.

and importance in general context of the orbital QPO models.

### 3 RELATIVISTIC SCALING OF ORBITAL FREQUENCIES AND BH QPOS

Characteristic periods  $T$  of geodesic orbital motion in strong gravity scale with the compact object mass  $M$ . Several models of QPOs, to which we in next refer as standard geodesic orbital (SGO) models, assume that the observed frequencies,  $\nu_L$  and  $\nu_U$ , are equal to frequencies of (geodesic) orbital motion represented by the Keplerian frequency of a circular orbit, by the radial and vertical epicyclic frequencies, or by their linear combinations (including the periastron and Lense-Thirring precession frequencies). These frequencies can be written in a general form

$$\nu_i = \frac{1}{T_i} = \frac{c^3}{2\pi G} \frac{1}{M} f_i(x, j, q), \quad (3)$$

where the orbital radius is rescaled as  $x = r/r_G$ ,  $r_G = GM/c^2$ ,  $j$  denotes the compact object (BH or NS) rotational parameter (dimensionless angular momentum),  $j = cJ/GM^2$ , and  $q$  stands for quadrupole moment,  $q = cQ/GM^3$ . The  $f_i$  function which determines given orbital frequency depends on  $j$  and  $q$ , but does not depend on  $M$ . For simplicity we from now on assume very compact objects (BH or dense NS),  $q \approx j^2$ .

In the specific case of the Keplerian frequency we can write the  $f$  function as (e.g. Bardeen et al. 1972; Abramowicz et al. 2003)

$$f_K = \frac{1}{x^{3/2} + j}. \quad (4)$$

An often quoted example of  $1/M$  scaling of the orbital frequencies is related to the innermost stable circular orbit. The Keplerian orbital frequency at this orbit around a Schwarzschild black hole,  $j = 0$ ,  $x_{ISCO} = 6$ , scales as (e.g. Kluzniak & Wagoner 1985)

$$\nu_{ISCO} = \frac{2.2 \text{ kHz}}{M^*}, \quad (5)$$

where  $M^* = M/M_\odot$ . For an extremely rotating Kerr black hole,  $j = 1$ ,  $x_{ISCO} = 1$ , the ISCO frequency is higher and one may write

$$\nu_{ISCO} = \frac{16.2 \text{ kHz}}{M^*}. \quad (6)$$

#### 3.1 Universal scaling of QPO frequencies in BH sources

It has been shown that the 3:2 frequencies observed in Galactic microquasars scale qualitatively in the same way as the above mentioned relations. The best fit of their data by the  $1/M$  relation has been determined as (McClintock & Remillard 2006a)

$$\nu_U = \frac{2.8 \text{ kHz}}{M^*}. \quad (7)$$

All Galactic microquasars therefore should have its rotational parameter similar to one another, except when the QPO frequencies are not much affected by its value (e.g. Török et al. 2007). For instance, the RP model predicts relation (7) for the observed 3:2 frequency ratio for  $j \sim 0.5$

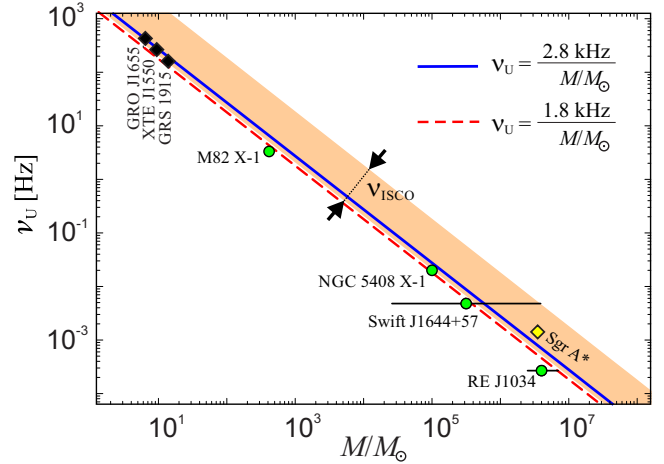


**Figure 1.** Large scaling of BH 3:2 QPO frequencies. The dashed line corresponding to  $\nu_U = 1.8 \text{ kHz}$  indicates the RP model prediction for the 3:2 frequency ratio and  $j = 0$ . The coloured region denotes the ISCO frequencies in the range of  $j \in [0, 1]$ .

(e.g. Török et al. 2011). On the other hand the Ep model predicts  $j \sim 0.9$  (Török et al. 2005).

It has been suggested that on a large range of  $M$  both the rotational parameter and specific details of a given orbital model are of secondary importance, and the observed frequencies can be used for the estimation of  $M$  (Abramowicz et al. 2004; Török 2005). At present there is a growing evidence for such a large range BH QPO frequencies scaling (Zhou et al. 2015). This is illustrated in Figure 1 which indicates the QPO data and expected BH masses investigated by Remillard et al. (2002); Remillard (2004); Pasham et al. (2014); Strohmayer et al. (2007); Reis et al. (2012); Gierliński et al. (2008); Aschenbach et al. (2004); Remillard & McClintock (2006); Reid et al. (2014); Huang et al. (2013); Miller & Gültekin (2011); Zhou et al. (2010); Gillessen et al. (2009). In the Figure 1 we include the  $\nu_U(M)$  relations associated to Keplerian frequency at ISCO as well as those predicted by the RP model. Further references and examples of other BH sources are discussed by Goluchová et al. (2019) and Gupta et al. (2019).

## 4 COMPARISON BETWEEN NS SOURCES

As we mentioned in Section 2, there are several competing QPO models that are still premature. It still is not clear whether the same model could be applied to both (BH and NS) classes of sources. The fixed frequencies of the weak BH QPOs seem to be in contrast with the variable frequencies of the often strong NS QPOs. It has been suggested within the framework of the SGO models that the fixed frequency ratio,  $R = 1.5$ , observed in the BH sources relates to a specific resonant orbit  $x_{3:2}$  (e.g. Török 2005). Local (e.g. the RP model) or global (e.g. the Ep model) oscillations of the accreted matter associated to this orbit have been shown to possibly evoke the observed variations of the flux in the BH sources (Bursa 2004; Schnittman & Bertschinger 2004; Bakala et al. 2015).

It has been proposed that physical mechanisms that occur at the NS boundary layer can enhance the observed

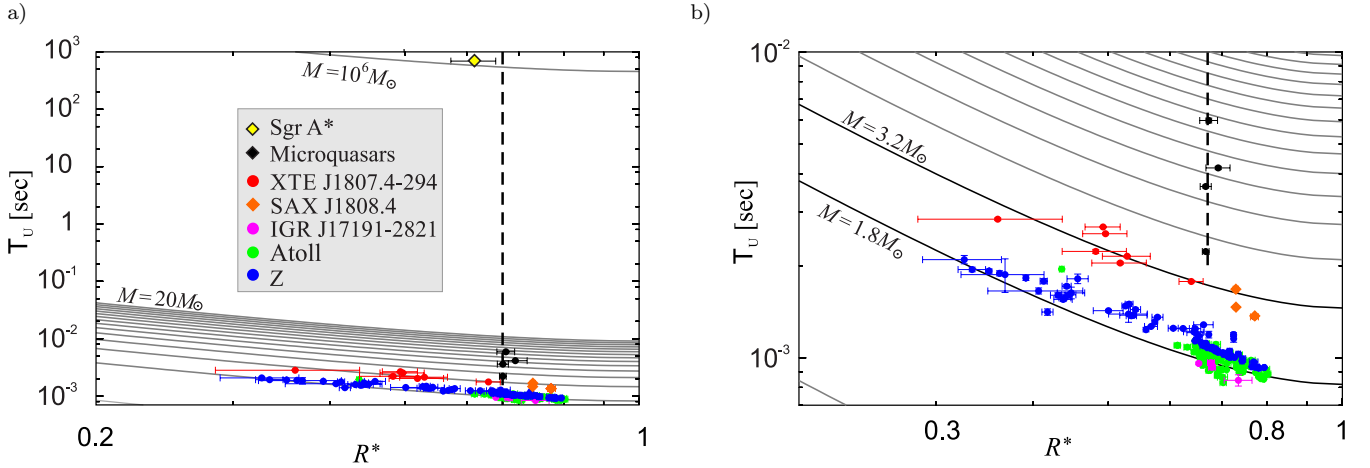


**Figure 2.** a) A comparison between the periods of BH and NS HF QPOs. The dashed vertical line corresponds to  $R = 1.5$ . The continuous lines indicate predictions of the RP model. In the bottom part of the plot the curves are spaced every 1.4 in  $M^*$ . b) An enlarged view of panel a.

variations of the flux in such a way that their amplitude is up to one order of magnitude higher than for the BH sources (Horák 2005; Abramowicz et al. 2007; Török et al. 2016b; Parthasarathy et al. 2017). The turbulent environment of the NS boundary layer can evoke variations of the QPO excitation radius. Within a possible unified BH-NS QPO model the presence of boundary layer and absence of event horizon can be responsible for the differences between BH and NS sources. One may naturally expect that in such model the  $1/M$  scaling of QPO frequencies found in BH sources should be manifested in the NS sources as well. We note that some  $1/M$  scaling may be expected in the NS sources even if the QPO mechanisms in the NS and BH sources were different provided that the mechanisms are described by some of the SGO models (that incorporate relativistic scaling of the orbital frequencies).

#### 4.1 Timescales

Within SGO class of models, the observed NS correlations  $\nu_U(\nu_L)$  can be related to a variable orbital radius  $x$  (e.g. Stella & Vietri 1998a,b). Assuming equation (3), for a fixed  $j$ , the ratio of QPO periods,  $R^*$ , depends only on  $x$  and not on  $M$ ,

$$R^* \equiv \frac{T_U}{T_L} = \frac{\nu_L}{\nu_U} = \frac{1}{R(x)}. \quad (8)$$

Moreover, for several models,  $R^*$  is a monotonic function of  $x$ .

Relations (3) and (8) imply that, for a fixed  $R^*$ , higher QPO periods correspond to a higher compact object mass. Having this motivation in mind, in Figure 2 we include QPO periods observed in the NS sources. Within the same Figure we also illustrate predictions of the RP model which implies  $r \rightarrow \infty$  when  $R^* \rightarrow 0$  and  $r \rightarrow r_{\text{ISCO}}$  when  $R^* \rightarrow 1$ . The NS sources included in Figure 2 are listed in Table 1.<sup>3</sup>

<sup>3</sup> We note that we do not consider Circinus X-1 in this paper because of the large extension of its  $R$  error bars (see Section 5.1 in Török et al. 2012).

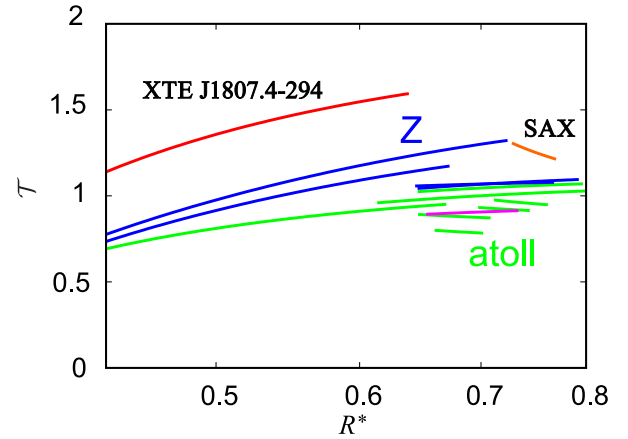


**Figure 3.** The  $\mathcal{T}(R^*)$  functions obtained for the individual sources and  $\bar{T}_U(R^*)$  inferred from the common fit of all data-points. The colour coding is the same as in Figure 2.

Inspecting Figure 2 we can find that, although there are some differences (see also Wang et al. 2014, 2018), both atoll and Z sources seem to roughly follow a common correlation  $T_U(R^*)$ . On the other hand, we can see that the XTE J1807.4-294 millisecond pulsar follows a correlation  $T_U(R^*)$  that is quantitatively different from that of the other displayed atoll and Z-sources except for SAX J1808.4-3658.

#### 4.2 Relative periods

We attempt to quantify the difference between XTE J1807.4-294 and other sources. We interpolate individual data of each of the 14 sources using relations (2) and (5) with best fitting coefficients  $\mathcal{M}$  and  $\mathcal{B}$ . In this way we obtain continuous correlations  $T_U(R^*)$  that well match the observational data.

We performed a common fit of data of all sources using relation (2). The fit ( $\mathcal{M} = 1.64 \pm 0.02$ ,  $\mathcal{B} = 0.67 \pm 0.01$ ) defines an averaged correlation  $\bar{T}_U(R^*)$  that can be used to

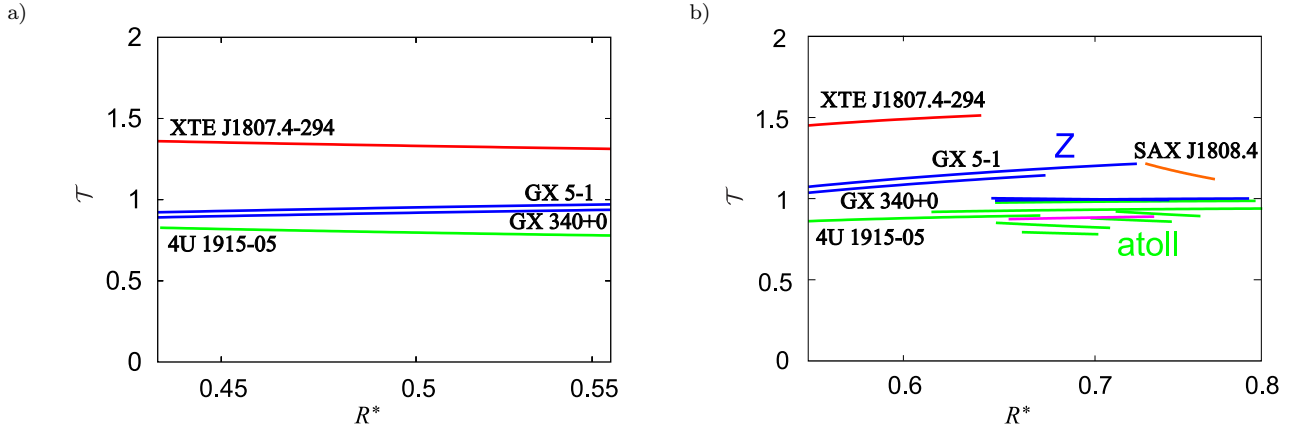


**Figure 4.** The  $\mathcal{T}(R^*)$  functions obtained for the individual sources and  $\bar{T}_U(R^*)$  given by relation (12). The colour coding is the same as in Figure 2. a) Results for the  $R_{\text{I}}^*$  interval. b) Results for the  $R_{\text{II}}^*$  interval.

explore the behaviour of relative periods

$$\mathcal{T} \equiv T_U / \bar{T}_U, \quad (9)$$

where individual continuous correlations  $T_U(R^*)$  interpolate individual data of each of the 14 sources using relations (2) and (5) with best fitting coefficients  $M$  and  $\mathcal{B}$ . The relative periods  $\mathcal{T}(R^*)$  obtained for each source are displayed in Figure 3. The Figure shows that the longest relative QPO periods of values close to  $\mathcal{T} \sim 1.5$  are reached for the XTE J1807.4-294 pulsar.

## 5 SCALING OF RELATIVE PERIODS WITH NS MASS

For a given source, neglecting the effects of NS rotation and assuming only SGO models,  $\mathcal{T}$  has to be a constant which only depends on  $M$ ,

$$\mathcal{T} = \mathcal{T}_0(M). \quad (10)$$

For the whole class of SGO models, there is

$$M = \tau \mathcal{T}_0 \mathcal{F}, \quad (11)$$

where  $\tau$  is the absolute period corresponding to  $\mathcal{T} = 1$  and  $\mathcal{F}$  is a factor specific for a given model. Consequently, a higher value of  $\mathcal{T}$  corresponds to a higher  $M$ .

### 5.1 Individual sources' behaviour

The curves drawn in Figure 3 clearly differ from constant functions. This can be an artefact of the application of common fit of data of all sources that was used to explore the behaviour of relative periods. In order to avoid bias connected to the non-uniform coverage of the QPO data along the large range of  $R^*$  we divide the examined data into two intervals,  $R_{\text{I}}^* \in [0.43, 0.56]$  and  $R_{\text{II}}^* \in [0.56, 0.8]$ . For the normalization of periods within the group of  $n$  sources we then consider an averaged correlation  $\bar{T}_U(R^*)$ ,

$$\bar{T}_U(R^*) = \sum_{N_o=1}^n T_U^{N_o}(R^*) / n, \quad (12)$$

instead of those given by the common fit. We note that there are only three datapoints available for SAX J1808.4-3658. These datapoints cover only a small part of the relevant interval and we exclude them from the calculation of  $\bar{T}$ . The  $\mathcal{T}(R^*)$  functions obtained for the two intervals of  $R^*$  are shown in Figure 4.

### 5.2 Distribution of $\mathcal{T}_0$

Figure 4 provides a rough quantitative comparison between different sources. Through approximation of the curves displayed within the  $R_{\text{II}}^*$  interval by straight lines, one can obtain a distribution of  $\mathcal{T}_0$  values. This specific distribution is illustrated in Figure 5a. The uncertainties related to individual values of  $\mathcal{T}_0$  within this distribution depend on very specific assumptions and could easily be underestimated.

In order to determine the value of  $\mathcal{T}_0$  and its uncertainty for each source in a rigorous and more robust way we analyze a full sample of data, as well as the individual sources separately, both across the whole range of  $R^*$ . Based on the fits obtained, we estimate mean values of  $\mathcal{T}_0$  that determine the relative mass of each source. We extract information on their uncertainties by performing Monte-Carlo simulations that provide 2-dimensional distributions of the fitting parameters  $\mathcal{M}$  and  $\mathcal{B}$ . The obtained results are given in Table 1 and illustrated in Figure 5b.

## 6 DISCUSSION AND CONCLUSIONS

The distribution of  $\mathcal{T}_0$  drawn in Figures 5a,b nicely illustrates the exceptionality of XTE J1807.4-294 - its characteristic QPO timescale is of a factor of 50% longer than the average timescale of other sources. For any SGO model and  $j = 0$  our finding implies that, compared to others, this source has a very high mass. We note that our conclusion is rather robust and does not depend on the exact form of formula (2) that we use to obtain the best data interpolation. For instance, when the formula is replaced by a simple linear term,  $\nu_L = a\nu_L + b$ , a very similar result is achieved, see Figures 5c,d.



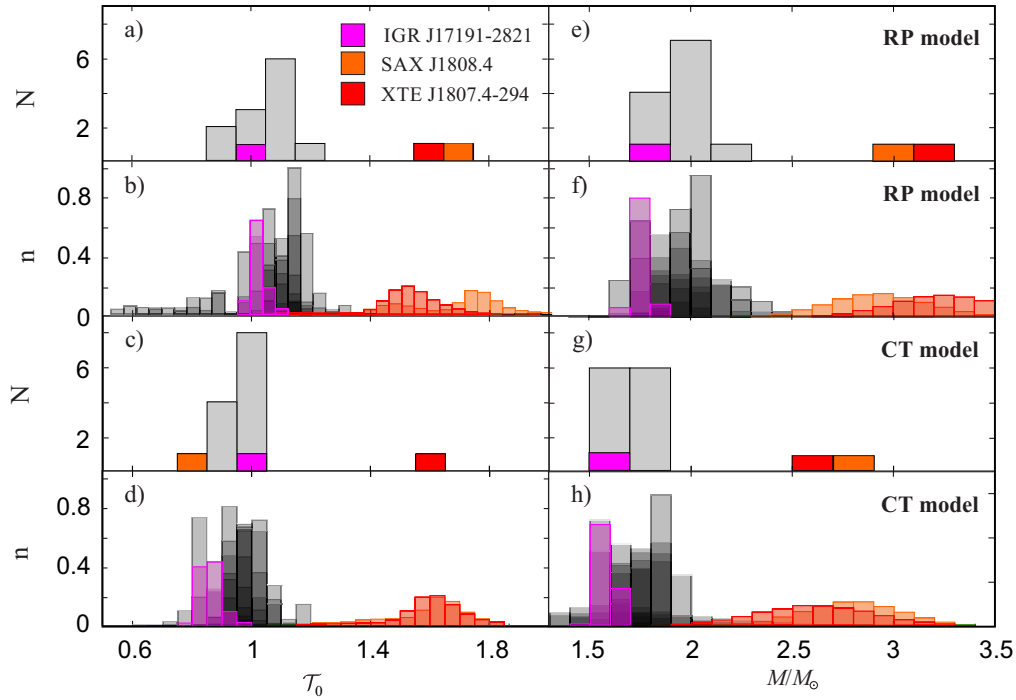


**Figure 5.** a) Distribution of  $\tau_0$  values associated to curves displayed in Figure 4b. The quantity  $N$  denotes the number of occurrences. b) Distribution of the estimated  $\tau_0$  values associated to individual sources drawn from Monte-Carlo simulations assuming 2-dimensional distributions in best fitting parameters given by relation (2). The quantity  $n$  denotes the relative number of occurrences. c) The same as in panel a), but made for the linear formula instead of relation (2). d) The same as in panel b), but made for the linear formula instead of relation (2). e) Distribution of NS mass implied by fitting the QPO data of the individual sources by the RP model for  $j = 0$ . f) A detailed estimation of uncertainties in NS mass drawn for the RP model,  $j = 0$ , and each source. g) Distribution of NS mass implied by fitting the QPO data of the individual sources by the CT model for  $j = 0$ . h) A detailed estimation of uncertainties in NS mass drawn for the CT model,  $j = 0$ , and each source.

An overall inspection of Figures 5a-d clearly supports our conclusion. We further illustrate this conclusion and display the NS mass distribution inferred from the RP and CT models and the XTE J1807.4-294 QPO data in Figures 5e-h that follows the results of Török et al. (2016b). It shows that for both QPO models and  $j = 0$  the inferred mass of the X-ray pulsar is indeed very high compared to other sources.

### 6.1 NS rotation and equation of state

In Figure 6 we illustrate NS mass and angular momentum as implied by fitting of the XTE J1807.4-294 QPO data by the RP and CT models for  $j \geq 0$ . Within the same Figure we include NS mass constraints following from several NS equations of state (EoS). These are namely EoS considered by Török et al. (2016b) - SLy 4, APR, AU-WFF1, UU-WFF2 and WS-WFF3 (Wiringa et al. 1988; Stergioulas & Friedman 1995; Akmal et al. 1998; Rikowska Stone et al. 2003), and two more EoS - L, l (Arnett & Bowers 1977; Urbanec et al. 2010). In this Figure we assume the NS rotational frequency of 191Hz reported by Linares et al. (2005); Boutloukos & Lamb (2008). The calculations were performed following the approach of Hartle & Thorne (1968), Chandrasekhar & Miller (1974), Miller (1977), Urbanec et al. (2013), Török et al. (2012) and Török et al. (2016b).

Inspecting Figure 6 we can see that the non-rotating NS mass implied by the RP model is rather high compared

to maximal non-rotating NS mass allowed by the assumed EoS. This is the case also for the CT model, even though this model implies considerably lower  $M$ . On the top of that, the estimated NS mass increases when NS rotation is taken into account. We note that such behavior is common for most SGO models (Török et al. 2016). For this reason it may be very difficult to match the long QPO periods in XTE J1807.4-294 when realistic models of rotating NS and SGO models are considered simultaneously.

Our findings on the SGO models and NS EoS are well illustrated by the example of the CT model shown in Figure 6b. EoS that allows for a very high NS mass is clearly required. In this sense we can state that the QPOs observed in XTE J1807.4-294 challenge the NS EoS.

### 6.2 Magnetic field

As apparent from Figure 2b datapoints of SAX J1808.4-3658 likely follow the same quantitative trend as datapoints of XTE J1807.4-294. One may speculate that the origin of very high  $\tau_0$  relies in a relatively strong pulsar magnetic field. This suggestion is in agreement with the scenario in which the magnetic field increases the gap between the accretion disc inner edge and the NS surface making the characteristic time scale of the orbital motion longer (see also Ghosh & Lamb 1978; Campbell 1992; Bakala et al. 2010, 2012; Habumugisha et al. 2018). Having said that, it is

**Table 1.** List of sources (A - atoll, Z - Z, P - AMXP) and obtained values of  $\tau_0$ . The uncertainties of  $\tau_0$  correspond to standard errors given by  $\tau_0$  distributions shown in Figure 5b. References: (1)–(3), (9) – (11) - Barret et al. (2005a,b, 2006), (4) - Boirin et al. (2000), (5) - Altamirano et al. (2010), (6) - Homan et al. (2002), (7) - Boutloukos et al. (2006), (8) - Linares et al. (2005), (12) - Jonker et al. (2000), (13) - Jonker et al. (2002), (14) - Bult & van der Klis (2015).

Source No./type	Name	$\tau_0$
1/A	4U 1608-52	$1.11 \pm 0.01$
2/A	4U 1636-53	$1.05 \pm 0.01$
3/A	4U 1735-44	$1.06 \pm 0.03$
4/A	4U 1915-05	$0.99 \pm 0.03$
5/A-P	IGR J17191-2821	$1.0 \pm 0.07$
6/Z	GX 17+2	$1.17 \pm 0.03$
7/Z	Sco X-1	$1.12 \pm 0.01$
8/A-P	XTE J1807.4-294	$1.58 \pm 0.20$
9/A	4U 1728-34	$0.96 \pm 0.03$
10/A	4U 0614+09	$1.06 \pm 0.03$
11/A	4U 1820-30	$1.11 \pm 0.03$
12/Z	GX 340+0	$0.90 \pm 0.16$
13/Z	GX 5-1	$0.91 \pm 0.26$
14/P	SAX J1808.4-3658	$1.80 \pm 0.94$

worth mentioning that datapoints of another AMXPs, IGR J17191-2821, follow the other sources. The exceptionality of the two sources therefore cannot be explained in terms of their magnetic field, at least not in a straightforward way.

## ACKNOWLEDGMENTS

We would like to acknowledge the Czech Science Foundation grant No. 17-16287S, the INTER-EXCELLENCE project No. LTI17018 supporting collaboration between the Silesian University in Opava and Astronomical Institute in Prague, and internal grants of the Silesian University in Opava, SGS/14,15/2016. We are grateful to Marek Abramowicz and Jiří Horák for useful discussions. Furthermore we would like to acknowledge the hospitality of the University of Oxford and the Astronomical Observatory in Rome. Last but not least, we express our sincere thanks to concierges of Mlýnská hotel in Uherské Hradiště for their kind help and participation in organizing frequent workshops of the Silesian university and the Astronomical institute.

## REFERENCES

Abramowicz M. A., Almergren G. J. E., Kluźniak W., Thampan A. V., 2003, ArXiv General Relativity and Quantum Cosmology e-prints  
 Abramowicz M. A., Barret D., Bursa M., Horák J., Kluźniak W., Rebusco P., Török G., 2005a, in Hledík S., Stuchlík Z., eds, RAGtime 6/7: Workshops on black holes and neutron stars A note on the slope-shift anticorrelation in the neutron star kHz QPOs data. pp 1–9  
 Abramowicz M. A., Barret D., Bursa M., Horák J., Kluźniak W., Rebusco P., Török G., 2005b, *Astronomische Nachrichten*, 326, 864  
 Abramowicz M. A., Blaes O. M., Horák J., Kluźniak W., Rebusco P., 2006, *Classical and Quantum Gravity*, 23, 1689  
 Abramowicz M. A., Bulik T., Bursa M., Kluźniak W., 2003a, *A&A*, 404, L21

Abramowicz M. A., Fragile P. C., 2013, *Living Reviews in Relativity*, 16, 1  
 Abramowicz M. A., Horák J., Kluźniak W., 2007, *Acta Astron.*, 57, 1  
 Abramowicz M. A., Karas V., Kluźniak W., Lee W. H., Rebusco P., 2003b, *PASJ*, 55, 467  
 Abramowicz M. A., Kluźniak W., 2001, *A&A*, 374, L19  
 Abramowicz M. A., Kluźniak W., McClintock J. E., Remillard R. A., 2004, *APJL*, 609, L63  
 Abramowicz M. A., Lanza A., Spiegel E. A., Szuszkiewicz E., 1992, *Nature*, 356, 41  
 Akmal A., Pandharipande V. R., Ravenhall D. G., 1998, *Phys. Rev. C*, 58, 1804  
 Alpar M. A., Shaham J., 1985, *Nature*, 316, 239  
 Altamirano D., Linares M., Patruno A., Degenaar N., Wijnands R., Klein-Wolt M., van der Klis M., Markwardt C., Swank J., 2010, *MNRAS*, 401, 223  
 Arnett W. D., Bowers R. L., 1977, *APJS*, 33, 415  
 Aschenbach B., Grosso N., Porquet D., Predehl P., 2004, *A&A*, 417, 71  
 Bakala P., Goluchová K., Török G., Šrámková E., Abramowicz M. A., Vincent F. H., Mazur G. P., 2015, *A&A*, 581, A35  
 Bakala P., Török G., Karas V., Dovčiak M., Wildner M., Wzientek D., Šrámková E., Abramowicz M., Goluchová K., Mazur G. P., Vincent F. H., 2014, *MNRAS*, 439, 1933  
 Bakala P., Urbanec M., Šrámková E., Stuchlík Z., Török G., 2012, *Classical and Quantum Gravity*, 29, 065012  
 Bakala P., Šrámková E., Stuchlík Z., Török G., 2010, *Classical and Quantum Gravity*, 27, 045001  
 Bardeen J. M., Press W. H., Teukolsky S. A., 1972, *APJ*, 178, 347  
 Barret D., Kluźniak W., Olive J. F., Paltani S., Skinner G. K., 2005, *MNRAS*, 357, 1288  
 Barret D., Olive J.-F., Miller M. C., 2005a, *MNRAS*, 361, 855  
 Barret D., Olive J.-F., Miller M. C., 2005b, *Astronomische Nachrichten*, 326, 808  
 Barret D., Olive J.-F., Miller M. C., 2006, *MNRAS*, 370, 1140  
 Barret D., Vaughan S., 2012, *AJ*, 746, 131  
 Belloni T. M., Altamirano D., 2013, *MNRAS*, 432, 10  
 Belloni T. M., Sanna A., Méndez M., 2012, *MNRAS*, 426, 1701  
 Boirin L., Barret D., Olive J. F., Bloser P. F., Grindlay J. E., 2000, *Astronomy and Astrophysics*, 361, 121  
 Boutloukos S., Lamb F. K., 2008, in Bassa C., Wang Z., Cumming A., Kaspi V. M., eds, 40 Years of Pulsars: Millisecond Pulsars, Magnetars and More Vol. 983 of American Institute of Physics Conference Series, Implications of kHz QPOs for the Spin Frequencies and Magnetic Fields of Neutron Stars: New Results from Circinus X-1. pp 533–535  
 Boutloukos S., van der Klis M., Altamirano D., Klein-Wolt M., Wijnands R., Jonker P. G., Fender R. P., 2006, *APJ*, 653, 1435  
 Bult P., van der Klis M., 2015, *APJ*, 806, 90  
 Bursa M., 2004, in Hledík S., Stuchlík Z., eds, RAGtime 4/5: Workshops on black holes and neutron stars Variability of accreting sources at very high time resolution. pp 25–32  
 Bursa M., 2005, in Hledík S., Stuchlík Z., eds, RAGtime 6/7: Workshops on black holes and neutron stars High-frequency QPOs in GRO J1655-40: Constraints on resonance models by spectral fits. pp 39–45  
 Campbell C. G., 1992, *Geophysical and Astrophysical Fluid Dynamics*, 63, 179  
 Chandrasekhar S., Miller J. C., 1974, *MNRAS*, 167, 63  
 de Avellar M. G. B., Porth O., Younsi Z., Rezzolla L., 2018, *MNRAS*, 474, 3967  
 Fragile P. C., Straub O., Blaes O., 2016, *MNRAS*, 461, 1356  
 Germanà C., 2017, *PRD*, 96, 103015  
 Germanà C., Kostić U., Cadež A., Calvani M., 2009, in Rodriguez J., Ferrando P., eds, American Institute of Physics Conference Series Vol. 1126 of American Institute of Physics Conference Series, Tidal Disruption of Small Satellites Orbiting Black Holes. pp 367–369  
 Ghosh P., Lamb F. K., 1978, *APJL*, 223, L83  
 Gierliński M., Middleton M., Ward M., Done C., 2008, *Nature*, 455, 369  
 Gillessen S., Eisenhauer F., Trippe S., Alexander T., Genzel R., Martins F., Ott T., 2009, *APJ*, 692, 1075  
 Goluchová K., Török G., Šrámková E., Abramowicz M. A., Stuchlík Z., Horák J., 2019, *A&A Lett.*, 622, L8

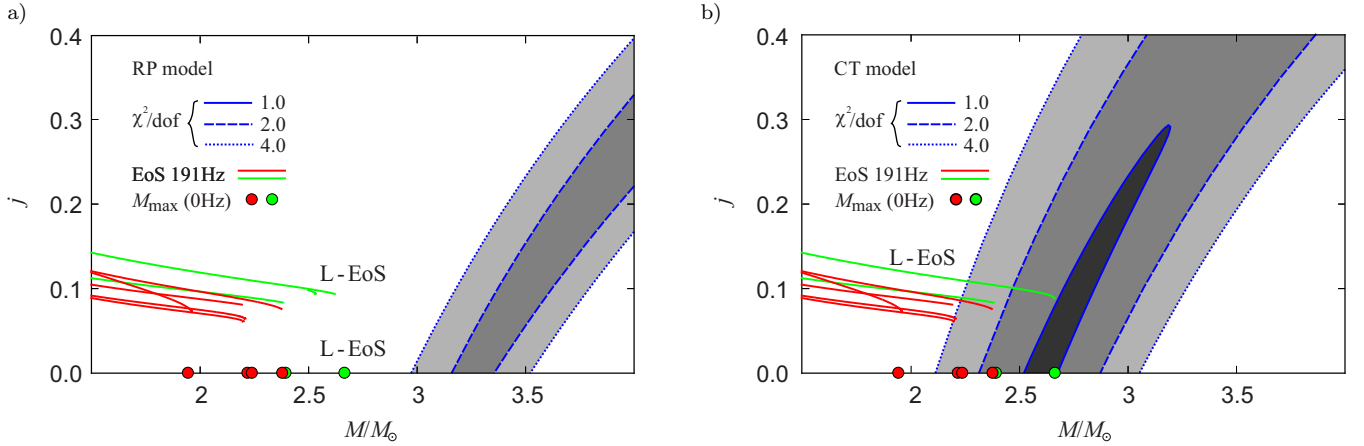


**Figure 6.** The mass–angular-momentum contours obtained from fitting of datapoints of XTE J1807.4-294 by QPO models vs. mass–angular-momentum relations predicted by models of rotating NSs. These are drawn for several NS EoS and spin 191Hz inferred from the X-ray burst measurements. The red colour corresponds to EoS assumed by Török et al. (2016b). Restrictions given by models assuming non-rotating NSs are also indicated. See Section 6.1 for details. a) RP model. b) CT model.

Gupta A. C., Tripathi A., Wiita P. J., Kushwaha P., Zhang Z., Bambi C., 2019, *MNRAS*, 484, 5785  
Habumugisha I., Jurua E., Tessema S. B., Simon A. K., 2018, *APJ*, 859, 147  
Hartle J. B., Thorne K. S., 1968, *AJ*, 153, 807  
Homan J., van der Klis M., Jonker P. G., Wijnands R., Kuulkers E., Méndez M., Lewin W. H. G., 2002, *The Astrophysical Journal*, 568, 878  
Horák J., 2005, *Astronomische Nachrichten*, 326, 845  
Huang C.-Y., Wang D.-X., Wang J.-Z., Wang Z.-Y., 2013, *Research in Astronomy and Astrophysics*, 13, 705  
Ingram A., Done C., 2010, *MNRAS*, 405, 2447  
Jonker P. G., van der Klis M., Homan J., Méndez M., Lewin W. H. G., Wijnands R., Zhang W., 2002, *MNRAS*, 333, 665  
Jonker P. G., van der Klis M., Wijnands R., Homan J., van Paradijs J., Méndez M., Ford E. C., Kuulkers E., Lamb F. K., 2000, *The Astrophysical Journal*, 537, 374  
Karssen G. D., Bursa M., Eckart A., Valencia-S M., Dovčiak M., Karas V., Horák J., 2017, *MNRAS*, 472, 4422  
Kato S., 2001, *PASJ*, 53, 1  
Kato S., 2007, *PASJ*, 59, 451  
Kato S., 2008, *PASJ*, 60, 111  
Kluźniak W., Abramowicz M. A., 2001, *ArXiv Astrophysics e-prints*  
Kluźniak W., Abramowicz M. A., Kato S., Lee W. H., Stergioulas N., 2004, *AJ*, 603, L89  
Kluźniak W., Wagoner R. V., 1985, *APJ*, 297, 548  
Kostić U., Čadež A., Calvani M., Gomboc A., 2009, *A&A*, 496, 307  
Lamb F. K., Shibazaki N., Alpar M. A., Shaham J., 1985, *Nature*, 317, 681  
Lattimer J. M., Prakash M., 2004, *Science*, 304, 536  
Linares M., van der Klis M., Altamirano D., Markwardt C. B., 2005, *APJ*, 634, 1250  
McClintock J. E., Remillard R. A., 2006a, *Black hole binaries*. pp 157–213  
McClintock J. E., Remillard R. A., 2006b, *Black hole binaries*. Cambridge University Press, pp 157–213  
Méndez M., Belloni T., 2007, *MNRAS*, 381, 790  
Miller J. C., 1977, *MNRAS*, 179, 483  
Miller J. M., Gültekin K., 2011, *APJL*, 738, L13  
Miller M. C., Lamb F. K., Psaltis D., 1998, *AJ*, 508, 791  
Mukherjee D., Bult P., van der Klis M., Bhattacharya D., 2015, *MNRAS*, 452, 3994  
Mukhopadhyay B., 2009, *AJ*, 694, 387  
Parthasarathy V., Kluźniak W., Čemeljić M., 2017, *MNRAS*, 470, L34  
Pasham D. R., Strohmayer T. E., Mushotzky R. F., 2014, *Nature*, 513, 74  
Patruno A., Watts A. L., 2012, *arXiv e-prints* 1206.2727

Pétri J., 2005, *A&A*, 439, L27  
Psaltis D., Belloni T., van der Klis M., 1999, *APJ*, 520, 262  
Psaltis D., Norman C., 2000, *ArXiv Astrophysics e-prints*  
Psaltis D., Wijnands R., Homan J., Jonker P. G., van der Klis M., Miller M. C., Lamb F. K., Kuulkers E., van Paradijs J., Lewin W. H. G., 1999, *AJ*, 520, 763  
Reid M. J., McClintock J. E., Steiner J. F., Steeghs D., Remillard R. A., Dhawan V., Narayan R., 2014, *APJ*, 796, 2  
Reis R. C., Miller J. M., Reynolds M. T., Gültekin K., Maitra D., King A. L., Strohmayer T. E., 2012, *Science*, 337, 949  
Remillard R. A., 2004, in Kaaret P., Lamb F. K., Swank J. H., eds, *X-ray Timing 2003: Rossi and Beyond Vol. 714 of American Institute of Physics Conference Series*, X-ray QPOs from Black Hole Binary Systems. pp 13–20  
Remillard R. A., McClintock J. E., 2006, *Annual Review of Astronomy & Astrophysics*, 44, 49  
Remillard R. A., Muno M. P., McClintock J. E., Orosz J. A., 2002, *APJ*, 580, 1030  
Rezzolla L., Yoshida S., Zanotti O., 2003, *MNRAS*, 344, 978  
Rikovska Stone J., Miller J. C., Konieczny R., Stevenson P. D., Strayer M. R., 2003, *Phys. Rev. C*, 68, 034324  
Schnittman J. D., Bertschinger E., 2004, *APJ*, 606, 1098  
Shi C., Li X.-D., 2009, *MNRAS*, 392, 264  
Shi C.-S., Zhang S.-N., Li X.-D., 2018, *MNRAS*  
Stella L., Vietri M., 1998a, in Paul J., Montmerle T., Aubourg E., eds, *19th Texas Symposium on Relativistic Astrophysics and Cosmology KHz Quasi Periodic Oscillations in Low Mass X-ray Binaries as Probes of General Relativity in the Strong Field Regime*. p. 315  
Stella L., Vietri M., 1998b, *APJL*, 492, L59  
Stella L., Vietri M., 1999, *Physical Review Letters*, 82, 17  
Stergioulas N., Friedman J. L., 1995, *AJ*, 444, 306  
Strohmayer T. E., Mushotzky R. F., Winter L., Soria R., Uttley P., Cropper M., 2007, *APJ*, 660, 580  
Stuchlík Z., Konar S., Miller J. C., Hledík S., 2008, *A&A*, 489, 963  
Stuchlík Z., Kotrlová A., Török G., 2013, *APJ*, 552, A10  
Stuchlík Z., Kotrlová A., Torok G., Goluchova K., 2014, *Acta Astron.*, 64, 45  
Stuchlík Z., Urbanec M., Kotrlová A., Török G., Goluchová K., 2015, *Acta Astron.*, 65, 169  
Titarchuk L., Wood K., 2002, *AJ*, 577, L23  
Török G., 2005, *A&A*, 440, 1  
Török G., Abramowicz M. A., Kluźniak W., Stuchlík Z., 2005, *A&A*, 436, 1  
Török G., Abramowicz M. A., Stuchlík Z., Šrámková E., 2007, in Hartkopf W. I., Harmanec P., Guinan E. F., eds, *Binary Stars as Critical Tools & Tests in Contemporary Astrophysics Vol. 240 of IAU Symposium*, QPOs in Microquasars: the Spin Problem. p. Harmanec



- Török G., Bakala P., Šrámková E., Stuchlík Z., Urbanec M., Goluchová K., 2012, *AJ*, 760, 138
- Török G., Goluchová K., Horák J., Šrámková E., Urbanec M., Pecháček T., Bakala P., 2016a, *MNRAS*, 457, L19
- Török G., Goluchová K., Horák J., Šrámková E., Urbanec M., Pecháček T., Bakala P., 2016b, *MNRAS*, 457, L19
- Török G., Goluchová K., Urbanec M., Šrámková E., Adámek K., Urbancová G., Pecháček T., Bakala P., Stuchlík Z., Horák J., Juryšek J., 2016, *The Astrophysical Journal*, 833, 273
- Török G., Goluchová K., Šrámková E., Horák J., Bakala P., Urbanec M., 2018, *MNRAS*, 473, L136
- Török G., Kotrlová A., Šrámková E., Stuchlík Z., 2011, *A&A*, 531, A59
- Török G., Stuchlík Z., Bakala P., 2007, *Cent. European J. of Phys.*, 5, 457
- Urbanec M., Béták E., Stuchlík Z., 2010, *Acta Astron.*, 60, 149
- Urbanec M., Miller J. C., Stuchlík Z., 2013, *MNRAS*, 433, 1903
- Čadež A., Calvani M., Kostić U., 2008, *A&A*, 487, 527
- van der Klis M., 2006, *Rapid X-ray Variability*. Cambridge University Press, pp 39–112
- Varniere P., Rodriguez J., 2018, *APJ*, 865, 113
- Wagoner R. V., 1999, *Phys. Reports*, 311, 259
- Wagoner R. V., Silbergleit A. S., Ortega-Rodríguez M., 2001, *AJ*, 559, L25
- Wang D. H., Chen L., Zhang C. M., Lei Y. J., Qu J. L., 2014, *Astronomische Nachrichten*, 335, 168
- Wang D. H., Chen L., Zhang C. M., Lei Y. J., Qu J. L., Song L. M., 2015, *MNRAS*, 454, 1231
- Wang D.-H., Zhang C.-M., Qu J.-L., Yang Y.-Y., 2018, *MNRAS*, 473, 4862
- Weber F., 1999, *Pulsars as Astrophysical Laboratories for Nuclear and Particle Physics*. CRC Press; 1 edition (May 1, 1999)
- Wiringa R. B., Fiks V., Fabrocini A., 1988, *Phys. Rev. C*, 38, 1010
- Zanotti O., Font J. A., Rezzolla L., Montero P. J., 2005, *MNRAS*, 356, 1371
- Zhang C., 2004, *A&A*, 423, 401
- Zhang C.-M., 2005, *Chinese J. of Astron. and Astrophys. Suppl.*, 5, 21
- Zhang C. M., Yin H. X., Zhao Y. H., Zhang F., Song L. M., 2006, *MNRAS*, 366, 1373
- Zhou X.-L., Yuan W., Pan H.-W., Liu Z., 2015, *APJL*, 798, L5
- Zhou X.-L., Zhang S.-N., Wang D.-X., Zhu L., 2010, *APJ*, 710, 16